Supporting Information

Boosting Multi-Center Luminescence in $Cs_7Cd_3Br_{13}$ via Synergistic Defect Passivation and Sensitization of Cu(I)

Jianjie Zhang [a], XinPeng Dai [a], Baocheng Luo [a], Qin Yan [a], Xing Fan [b], Liumei Su*, [a]

a. Guangxi Key Laboratory of Advanced Rare Earth Materials, School of Resources, Environment and Materials, Guangxi University, Nanning, 530004, P.R. China. E-mail address: suliumei2020@gxu.edu.cn.

b. School of Materials and Environment, Guangxi Key Laboratory of Advanced Structural Materials and Carbon Neutralization, Guangxi Colleges and Universities Key Laboratory of Eco-friendly Materials and Ecological Restoration, Guangxi Minzu University, Nanning, 530105, PR China.

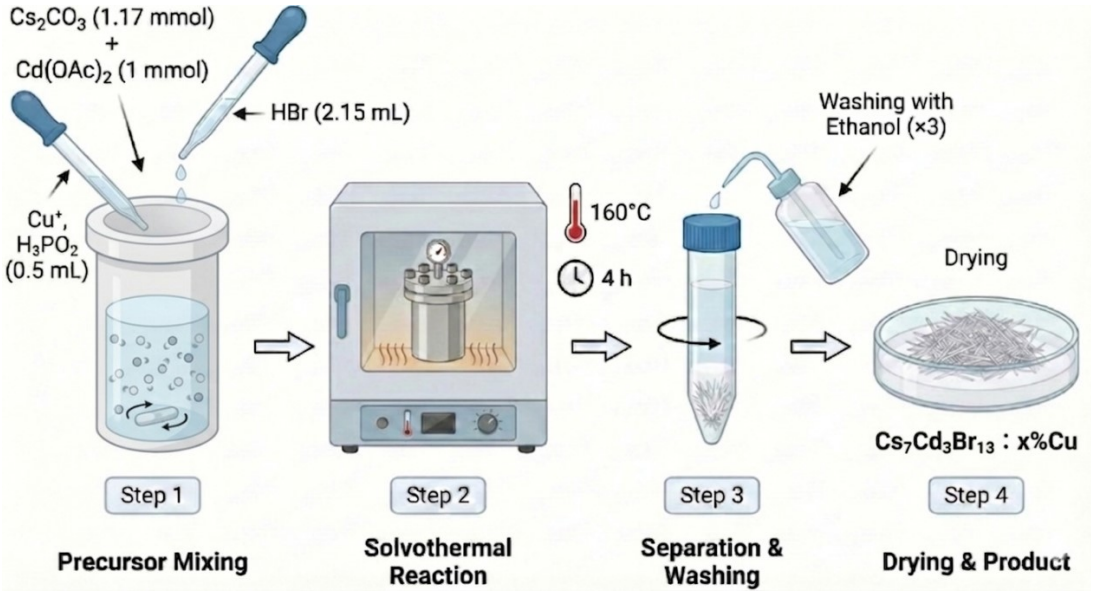

Figure S1. Schematic illustration of sample preparation.

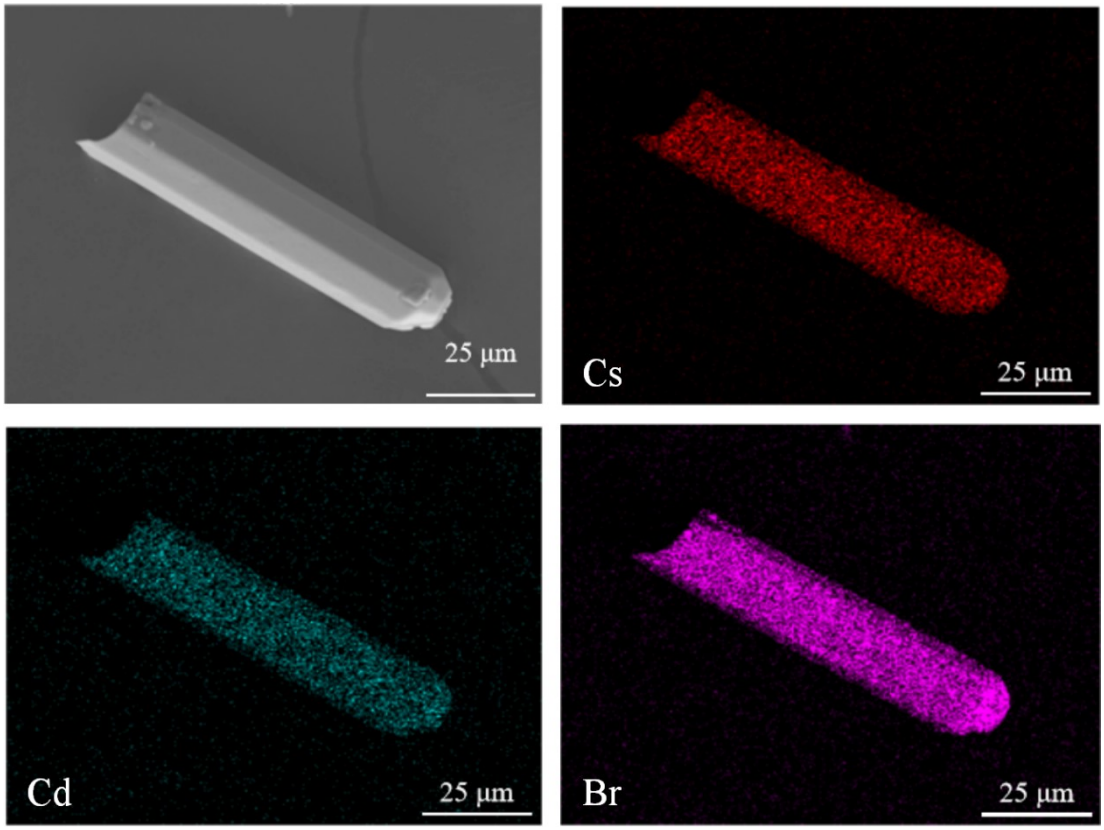

Figure S2. The SEM image and EDS-mapping of $Cs_7Cd_3Br_{13}$.

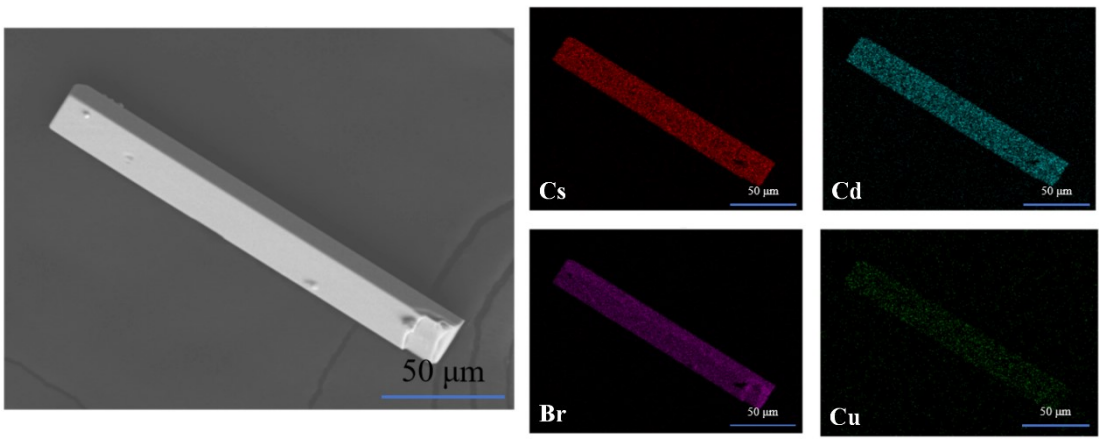

Figure S3. The SEM image and EDS-mapping of $Cs_7Cd_3Br_{13}$:0.07%Cu^+.

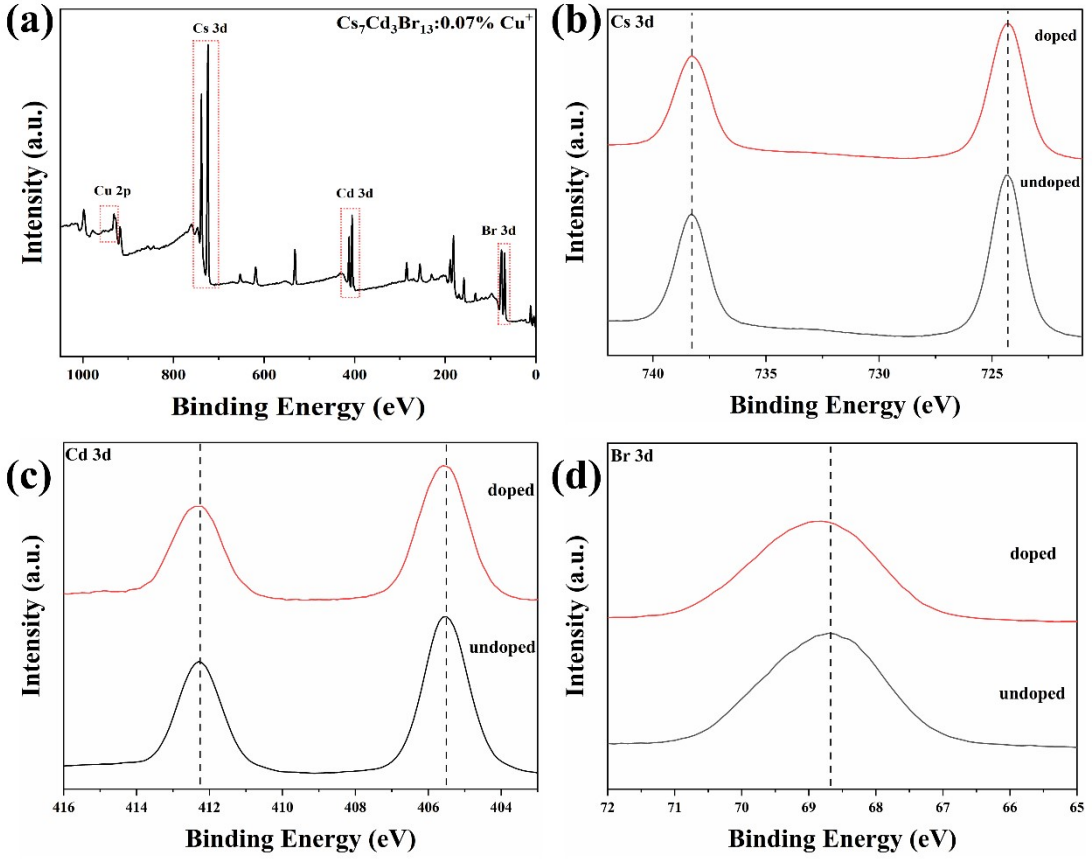

Figure S4. (a) XPS spectrum of $Cs_7Cd_3Br_{13}$:0.07%Cu. High-resolution XPS spectra of (b) Cs, (c) Cd, and (d) Br in $Cs_7Cd_3Br_{13}$ and $Cs_7Cd_3Br_{13}$:0.07%Cu.

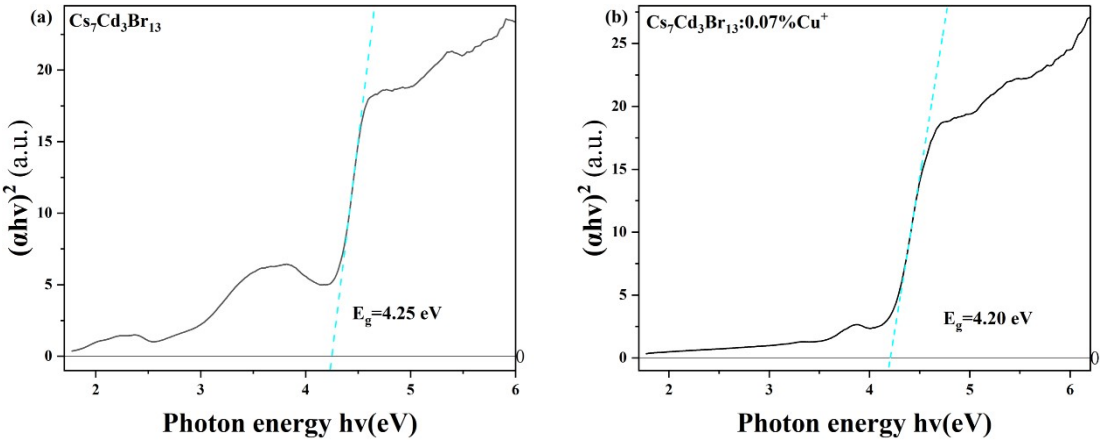

Figure S5. Tauc plots fo (a) $Cs_7Cd_3Br_{13}$ and (b) $Cs_7Cd_3Br_{13}$:0.07%Cu^+.

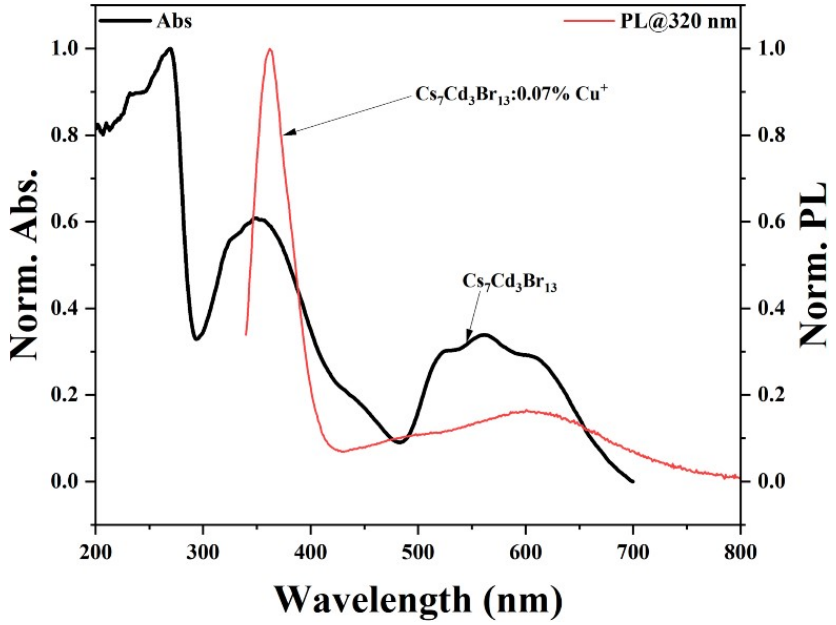

Figure S6. Normalized UV-vis absorption (black) and PL spectra (red, λ_{ex} = 320 nm) of $Cs_7Cd_3Br_{13}$ and $Cs_7Cd_3Br_{13}$:0.07%Cu^+.

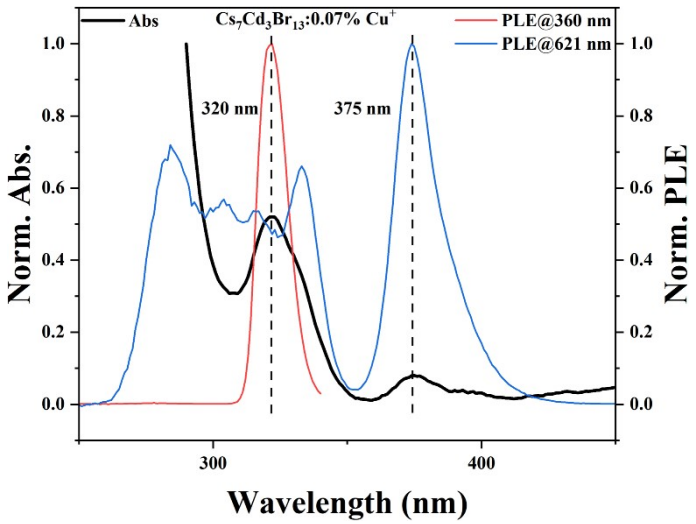

Figure S7. Comparison of the magnified absorption-edge tail and the normalized PLE spectra (monitoring at 360 and 621 nm) for $Cs_7Cd_3Br_{13}$:0.07%Cu^+

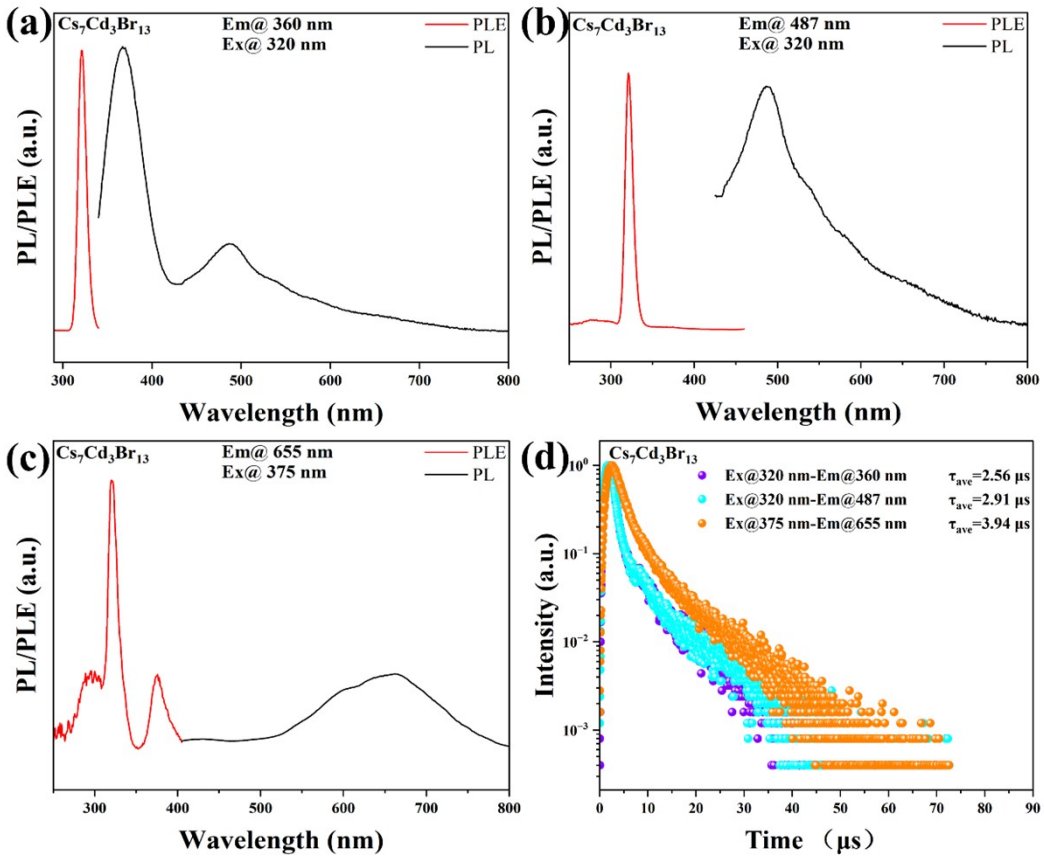

Figure S8. PLE and PL spectra of $Cs_7Cd_3Br_{13}$ (a) Em = 360 nm, Ex = 320 nm, (b) Em = 487 nm, Ex = 320 nm. and (c) Em = 655 nm, Ex = 375 nm. (d) PL decay curves of $Cs_7Cd_3Br_{13}$.

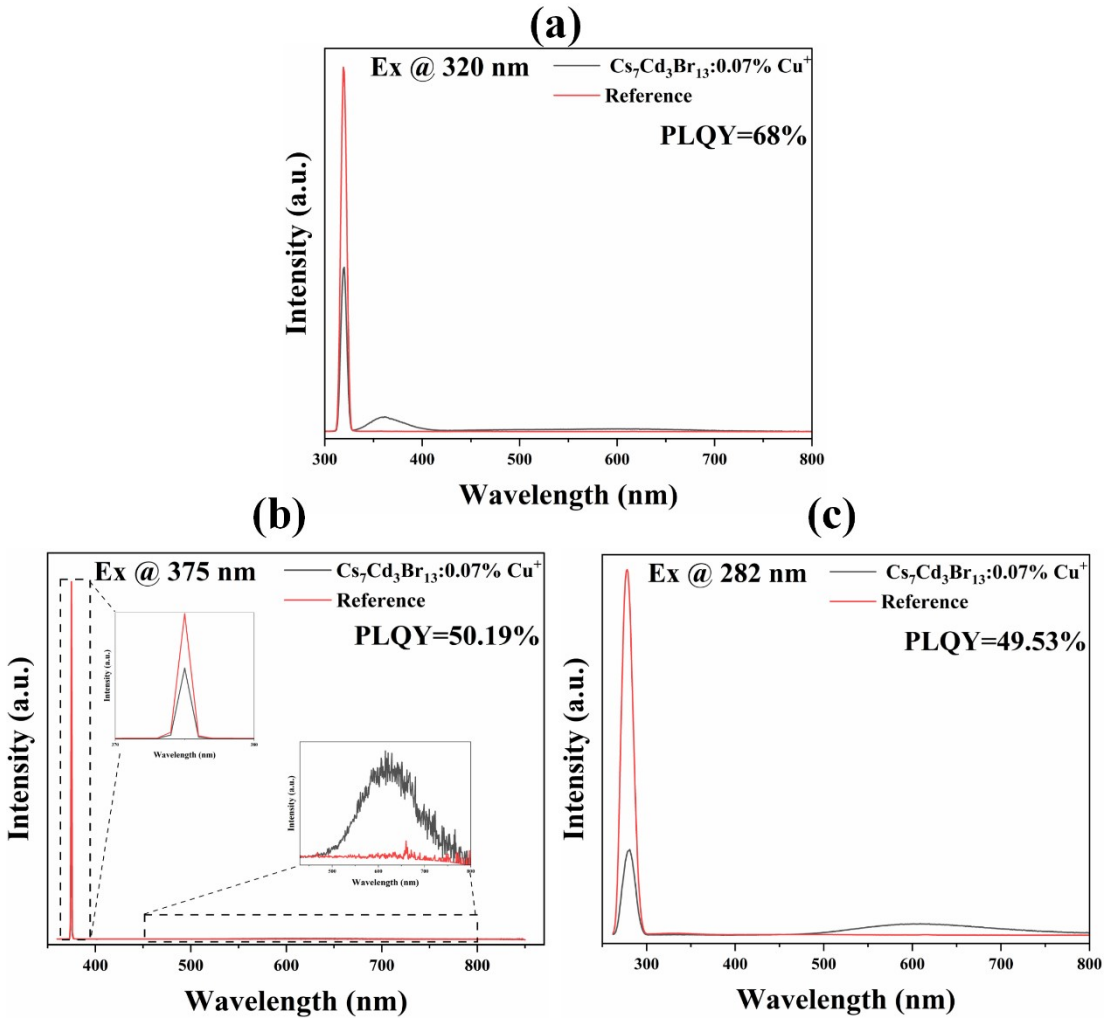

Figure S9. Photoluminescence quantum yield measurements of $Cs_7Cd_3Br_{13}$:0.07%Cu^+ under different excitation wavelengths: (a) λ_{ex} = 320 nm, (b) λ_{ex} =375 nm, and (c) λ_{ex} =282 nm.

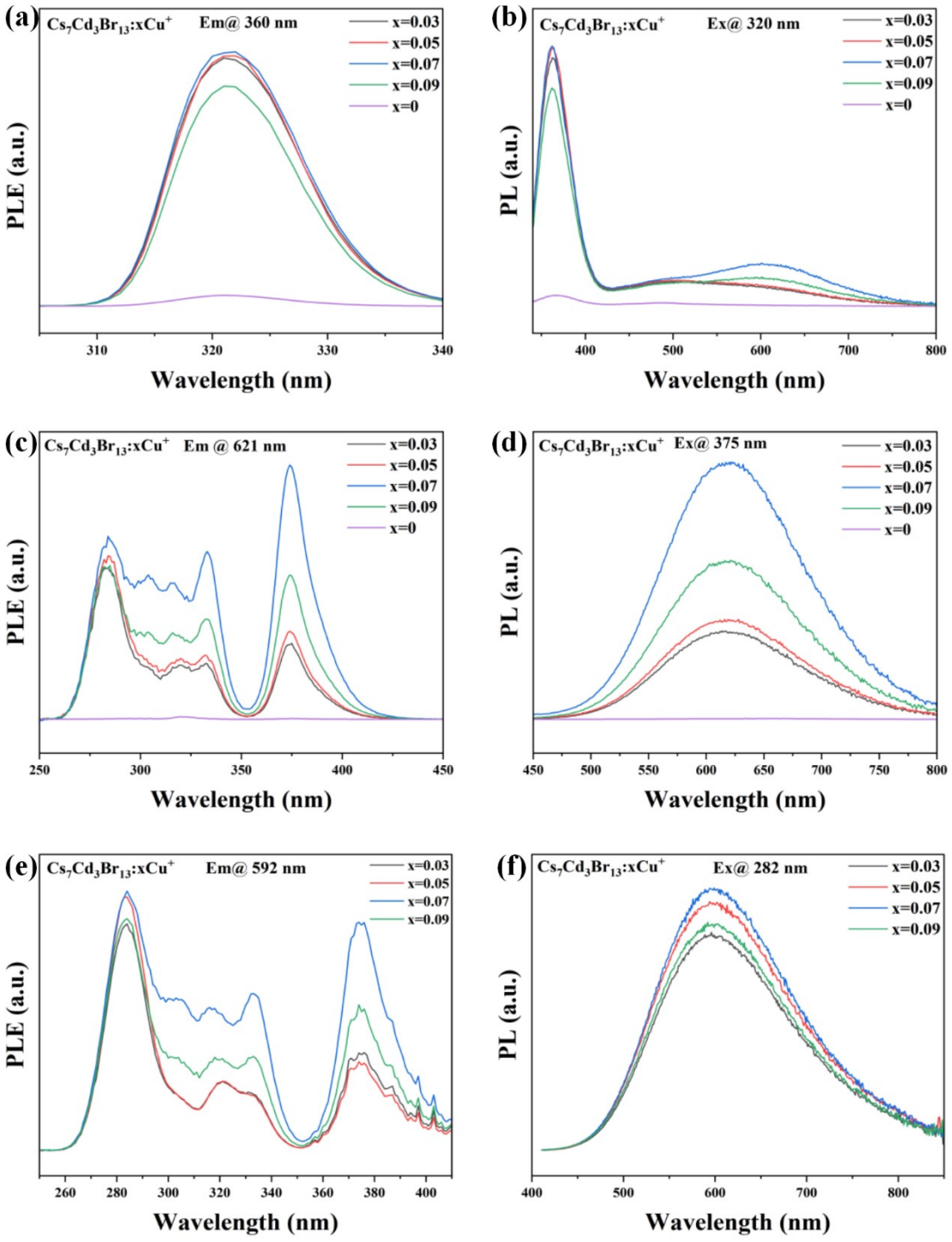

Figure S10. The PLE spectra monitored at (a) 360, (c) 621, and (e) 592 nm, as well as the PL spectra excited at (b) 320, (d) 375, and (f) 292 nm for $Cs_7Cd_3Br_{13}$:xCu^+.

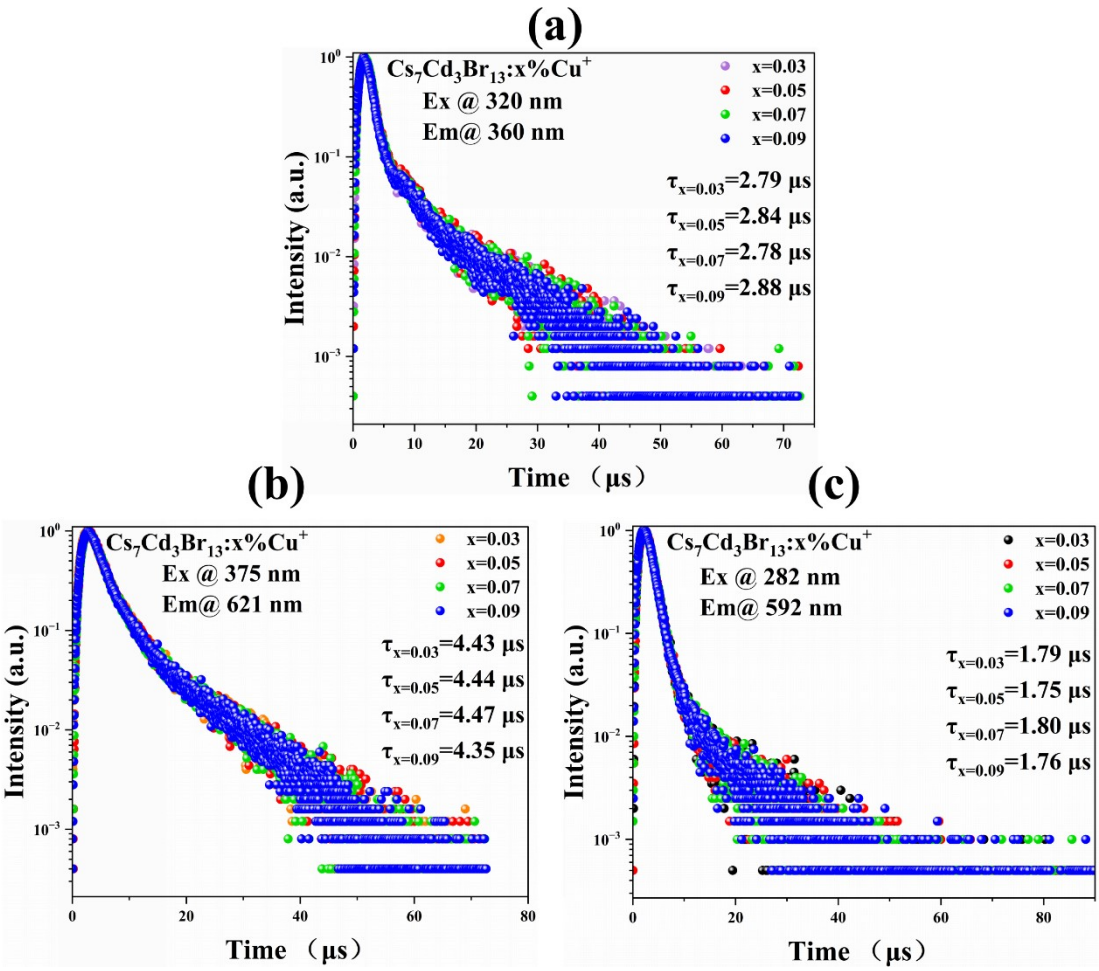

Figure S11. PL decay curve of $Cs_7Cd_3Br_{13}$:0.07%Cu^+. (a)λ_{ex} = 320 nm;(b) λ_{ex} = 375 nm;(c) λ_{ex} = 282 nm)

Table S1. Comparison of fluorescence lifetimes before and after doping with Cu^+ in the sample.

	$\tau_{360\ nm}$	$\tau_{621\ nm}$
Before Cu^+ doping	2.56 μs	3.94 μs
After Cu^+ doping	2.78 μs	4.47 μs

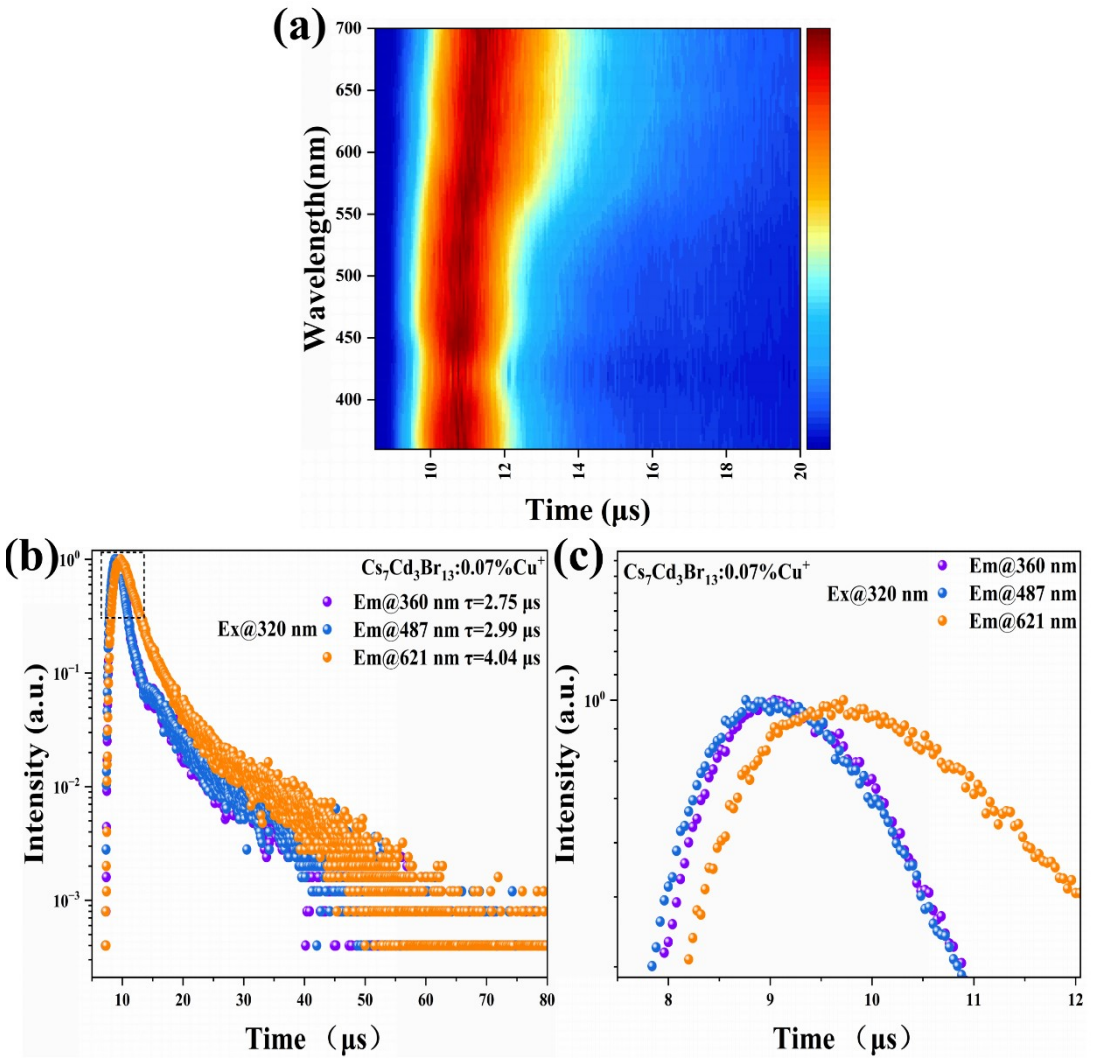

Figure S12. Time-resolved photoluminescence of $Cs_7Cd_3Br_{13}$:0.07%Cu^+ under 320 nm excitation: (a) Time-resolved emission spectrum. (b) Comparison of decay curves, and (c) Zoomed-in early-time dynamics at selected emission wavelengths.

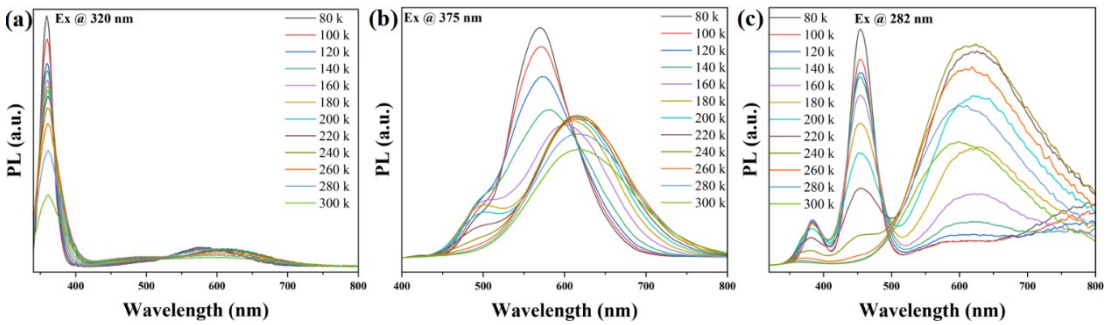

Figure S13. Temperature-dependent PL spectra of $Cs_7Cd_3Br_{13}$:0.07%Cu^+ recorded from 80 to300 K under excitation at (a)320 nm, (b)375 nm, and (c)282 nm.

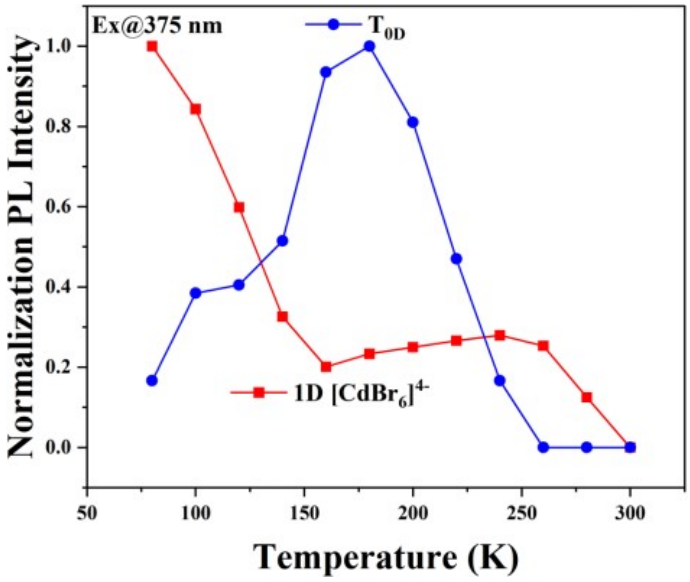

Figure S14. Temperature-dependent normalized PL intensities of two emission components under the same excitation (λ_{ex} = 375 nm) assigned to T_{0D} and 1D $[CdBr_6]^{4-}$ units.

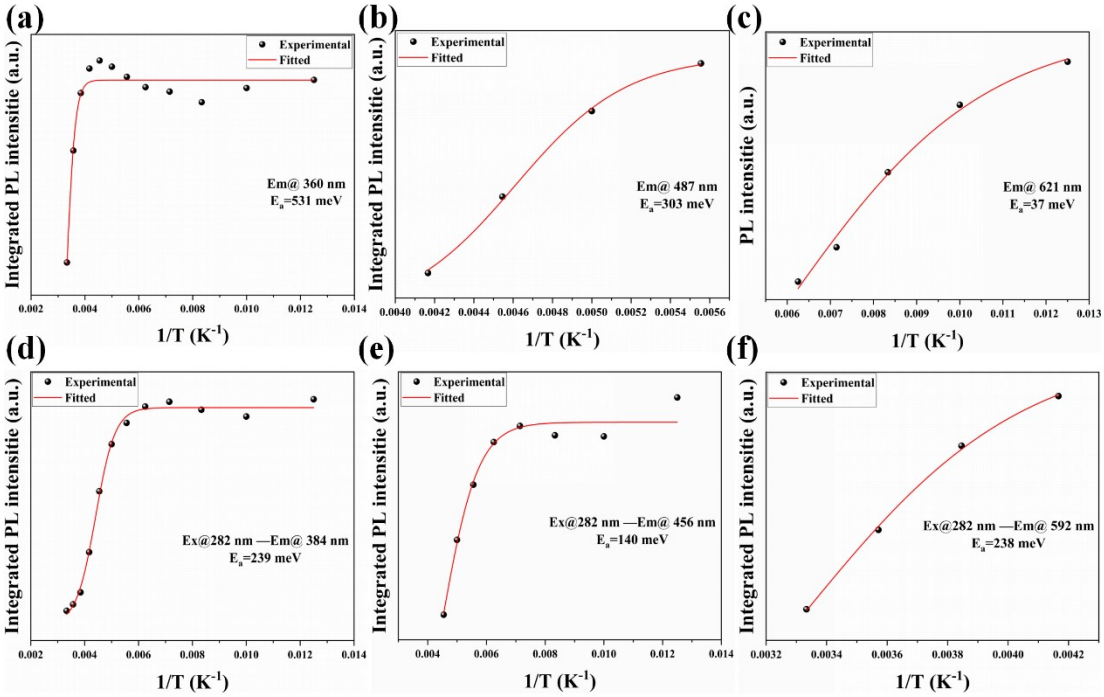

Figure S15. Dependence of the integrated PL intensities on 1/T of $Cs_7Cd_3Br_{13}$:0.07%Cu^+

Table S2. Comparison of the photoluminescence characteristics of the present Cu^{+}-doped $Cs_7Cd_3Br_{13}$ with those of previously reported related low-dimensional metal halides, including emission wavelength/range, FWHM, PLQY, and representative luminescence behaviors.

Material	Emission peak / range (nm)	FWHM (nm)	PLQY (%)	Characteristic feature / application	Ref.
$Cs_7Cd_3Br_{13}$:Cu	340–800	/	68	Single-component ultrabroadband visible emission	This work
	621	143	49.5	Robust orange emission; excitation-dependent PL	
	592	174	50.1	Temperature-dependent multiband emission	
$Cs_7Cd_3Br_{13}$:Sb	625	110	57.6	Robust orange emission	1
$Cs_7Cd_3Br_{13}$:Mn	577	85	50	Robust Yellow emission	2
$Cs_7Cd_3Br_{13}$:Mn/Pb	350–700	/	98	white light emitters	3
$Cs_7Cd_3Br_{13}$:Mg/Mn	590	80	45.9	Thermochromic luminescence	4
$Cs_7Cd_3Br_{13}$:Pb/Sb	350–700	/	93.7	X-ray imaging, lighting, optical encryption	5
$Cs_7Cd_3Br_{13}$:Pb/Sb	380-800	/	17.2	excitation-dependent PL	6
Cs_2AgBr_3:Cu	506	159	21.4	Cyan emission	7
$(MA)_2ZnCl_4$:Cu	486	75	54.9	Blue LED	8
$Cs_3Cd_2Cl_7$:Cu	560	150	81.6	X-ray inspection.	9
Cs_2ZnCl_4:Cu	480	71.54	35.2	cyan emission	10

References

1 T. Chang, Q. Wei, Z. Wang, Y. Gao, B. Lian, X. Zhu, S. Cao, J. Zhao, B. Zou and R. Zeng, *J. Phys. Chem. Lett.*, 2022, **13**, 3682–3690.

2 C. Yang, B. Ke, Q. Wei, S. Ge, B. He, X. Zhong and B. Zou, *Inorg. Chem.*, 2023, **62**, 3075–3083.

3 M. Gao, Y. Pan, C. Peng, Y. Ding, H. Lian, L. Li and J. Lin, *Chem. Mater.*, 2023, **35**, 773–782.

4 W. Liao, X. Zhou, J. Jin, Y. Wang and Z. Xia, *Laser & Photonics Reviews*, 2024, **18**, 2400194.

5 T. Chang, L. Wang, T. Kou, Q. Wei, P. Li, S. Han, F. Nan, X. Li, D. Huang, R. Zeng, Z. Chen and W. W. Yu, *Carbon Energy*, 2025, **7**, e70016.

6 B. Zheng, S. Ge, L. Chen, Y. Wen, K. Huang and B. Zou, *Nanomaterials*, 2025, **15**, 1238.

7 R. Fan, X. Zhang, J. Qiao, J. Xu, S. Feng and G. Liu, *Journal of Luminescence*, 2025, **279**, 121048.

8 Y. Bai, S. Zhang, N. Luo, B. Zou and R. Zeng, *Nano Res.*, 2024, **17**, 7768–7775.

9 T. Ye, Y. Wang, Z. Gao, S. Ge, H. Qin, X. He, J. Wu, R. Liu, M. Zhu, T. Zhou, Z. Pan, J. Hou, M. Wang, Y. He, L. Wang, H. Chen and W. Jiang, *ACS Appl. Opt. Mater.*, 2025, **3**, 898–907.

10 J. Chen, X. Zhu, T. Zhao, D. Geng, L. Huan, X. Yang, J. Li and Y. Deng, *ACS Appl. Mater. Interfaces*, 2026, **18**, 16863–16871.